Pediatric RESEARCH

BASIC SCIENCE ARTICLE

TNFα-stimulated protein 6 (TSG-6) reduces lung inflammation in an experimental model of bronchopulmonary dysplasia

Carleene Bryan[1], Ibrahim Sammour[1], Kasonya Guerra[1], Mayank Sharma[1], Fredrick Dapaah-Siakwan[1], Jian Huang[1], Ronald Zambrano[1], Merline Benny[1], Shu Wu[1] and Karen Young[1]

BACKGROUND: Inflammation is a key factor in the pathogenesis of bronchopulmonary dysplasia (BPD). Tumor necrosis factor–stimulated protein 6 (TSG-6) is a glycoprotein that modulates inflammation. Here we tested the hypothesis that intratracheal (IT) administration of an adenovirus overexpressing TSG-6 (AdTSG-6) would decrease inflammation and restore lung structure in experimental BPD.

METHODS: Newborn Sprague-Dawley rats exposed to normoxia (RA) or hyperoxia (85% O_2) from postnatal day (P) 1–P14 were randomly assigned to receive IT AdTSG-6 or placebo (PL) on P3. The effect of IT AdTSG-6 on lung inflammation, alveolarization, angiogenesis, apoptosis, pulmonary vascular remodeling, and pulmonary hypertension were evaluated on P14. Data were analyzed by two-way ANOVA.

RESULTS: TSG-6 mRNA was significantly increased in pups who received IT AdTSG-6. Compared to RA, hyperoxia PL-treated pups had increased NF-kβ activation and lung inflammation. In contrast, IT AdTSG-6 hyperoxia-treated pups had decreased lung phosphorylated NF-kβ expression and markers of inflammation. This was accompanied by an improvement in alveolarization, angiogenesis, pulmonary vascular remodeling, and pulmonary hypertension.

CONCLUSIONS: IT AdTSG-6 decreases lung inflammation and improves lung structure in neonatal rats with experimental BPD. These findings suggest that therapies that increase lung TSG-6 expression may have beneficial effects in preterm infants with BPD.

Pediatric Research (2019) 85:390–397; https://doi.org/10.1038/s41390-018-0250-2

INTRODUCTION

Bronchopulmonary dysplasia (BPD) is characterized by alveoli simplification and disordered angiogenesis.[1] Despite significant advancements in the field of neonatology, BPD continues to be one of the most common causes of respiratory morbidity and mortality in very low birth weight infants.[2] According to data from the National Institute of Child Health and Development, during the years 2003–2007, the incidence of BPD in infants <29 weeks gestational age was 42%,[3] with an increasing trend over the past 10 years.[4] Effective preventative and therapeutic strategies are therefore urgently needed.

Inflammation resulting from mechanical ventilation, oxygen toxicity, and infection is a key factor in the pathogenesis of BPD.[5] Multiple pro-inflammatory and chemotactic factors are present in the tracheal aspirates of infants who subsequently develop BPD,[6] and this inflammatory milieu initiates a cascade of events that result in an arrest of alveolar and vascular development.[5] Tumor necrosis factor (TNF)–stimulated protein 6 (TSG-6) is a 35-kDa glycoprotein that plays a key role in modulating the inflammatory response.[7] While most published reports show sparse constitutive TSG-6 expression in adult tissue, there is evidence that TSG-6 is constitutively expressed in bronchial epithelial cells, unstimulated neutrophils, epidermal cells, and brain tissue.[8–10] In response to pro-inflammatory mediators, TSG-6 levels are, however, increased in several cells, including macrophages, mesenchymal stem cells, monocytes, and myeloid dendritic cells.[8,11,12] TSG-6 is also elevated in the serum of animals with severe burns and the crush-injured spinal cord of rodents.[9,13] Moreover, TSG-6 expression is induced in mechanically stimulated smooth muscle cells[14] and in cultured chondrocytes following exposure to growth factors such as transforming growth factor-β and platelet-derived growth factor.[15]

Although the molecular mechanisms underlying the anti-inflammatory properties of TSG-6 are not entirely clear, there is evidence that TSG-6 inhibits components in the inflammatory network of proteases and suppresses neutrophil migration into sites of inflammation.[16] TSG-6 also participates in extracellular matrix remodeling by interacting with glycosaminoglycans, such as hyaluronan and the serine protease inhibitor, inter-alpha-inhibitor.[17] In addition, TSG-6 binds to CD44 on inflammatory cells either directly or in a complex with hyaluronan and this results in dissociation of CD44 from Toll-like receptors 2 and 4 (TLR-2, TLR-4), thereby limiting TLR-driven nuclear factor-kβ (NF-kβ) pro-inflammatory signaling.[18]

Although increased (NF-kβ) pro-inflammatory signaling is evident in lung diseases,[19] the role of TSG-6 in the pathogenesis of BPD has been less explored. TSG-6 is implicated in the propagation of eosinophilic pulmonary inflammation but intravenous administration of TSG-6 in rodents with bleomycin-induced lung fibrosis decreases inflammatory cell infiltration and improves

[1]Department of Pediatrics, University of Miami Miller School of Medicine, Miami, FL, USA
Correspondence: Karen Young (kyoung3@med.miami.edu)

Received: 3 July 2018 Accepted: 15 November 2018
Published online: 11 December 2018

survival.[20,21] In chemically injured corneas, administration of recombinant human TSG-6 dose-dependently decreases corneal opacity, neovascularization, and neutrophil infiltration[22] and knockdown of TSG-6 in mesenchymal stem cells attenuates its anti-inflammatory properties.[13]

Given recent studies suggesting that the lung protective of mesenchymal stem cells in experimental BPD may be mediated by TSG-6,[23] we tested the hypothesis that intra-tracheal (IT) administration of an adenovirus overexpressing human TSG-6 (AdTSG-6) would suppress lung inflammation and improve lung structure in experimental BPD. We show that TSG-6 is expressed in the developing lung and IT AdTSG-6 decreases lung phosphorylated NF-kβ expression, reduces inflammatory cytokine expression, and improves lung structure in rodents with experimental BPD. These findings suggest a potential role of TSG-6 in modulating the inflammatory milieu in the developing premature lung.

METHODS

Animals

Pregnant Sprague-Dawley rats were purchased from Charles River Laboratories (Wilmington, MA) and cared for according to National Institute of Health guidelines for use and care of animals. The experimental protocol was approved by the Animal Care and Use Committee of the University of Miami Miller School of Medicine. Rats were housed in a temperature-regulated room. Their chambers were cleaned twice weekly and food and water replaced as needed.

Experimental procedure

Newborn Sprague-Dawley pups from four litters were assigned at birth to room air (RA) or hyperoxia (85% O_2) from postnatal day (P) 1 to P14. Pups were housed in a plexiglass chamber with O_2 monitoring. The litter for each experimental group was limited to 10 pups to control for the effect of litter size on nutrition and growth. Males and females were evenly distributed among the groups. Dams were rotated every 48 h to standardize the nutrition provided to each litter. Oxygen exposure was continuous with brief intermittent interruptions to allow for animal care. After 2 weeks of the designated exposure, the litters were removed and hemodynamic and morphometric measurements obtained.

AdTSG-6 administration

Rat pups exposed to hyperoxia or RA from P1 to P14 were randomly assigned to receive IT AdTSG-6 (Vector Labs, Burlingame, CA) or adenovirus-expressing green fluorescent protein as placebo (PL) on P3. On P3, the pups were anesthetized with inhaled isoflurane (2–4%) and the trachea exposed through a small midline incision in the neck. AdTSG-6 (2×10^6 plaque-forming unit (PFU)/50 µl) or PL (50 µl) was delivered by tracheal puncture with a 30-gauge needle. Pups were placed in a warmed plastic chamber under RA or hyperoxic conditions for recovery. Once the pups were fully awake, they were returned to their respective dams. The dose was chosen based on pilot studies in our laboratory.

Assessment of pulmonary hypertension (PH)

Right ventricular systolic pressure (RVSP) was evaluated as a surrogate of pulmonary artery pressure. A thoracotomy was performed and a 22-gauge needle connected to a pressure transducer was inserted into the right ventricle of P14 pups. RVSP was measured and recorded on a Gould polygraph (model TA-400; Gould Instruments, Cleveland, OH) as previously described.[24]

Assessment of lung alveolarization

Lung morphometry was performed as previously described.[24] Serial 5-µm-thick paraffin-embedded sections were stained with hematoxylin and eosin. Images from 10 randomly selected, non-overlapping parenchymal fields were acquired from one lung section of each animal at ×20 magnification by a blinded observer. Alveolarization was determined by measuring the mean linear intercept (MLI) and radial alveolar count (RAC) as previously described.[25,26]

Assessment of vascular density

Vascular density was evaluated using 5-µm-thick lung sections of the upper and lower lobes that were deparaffinized, rehydrated, and stained with polyclonal rabbit anti-human von Willebrand Factor (vWF; 1:200, Dako Corp, Carpentaria, CA) and 4′6-di-amidino-2-phenylindole (DAPI; Vector Laboratories, Burlingame, CA). Five randomly selected, non-overlapping parenchymal fields were evaluated from lung sections of each animal. A blinded observer counted the number of vWF-positive (vWF^{pos}) blood vessels (20–50 µm) in each high-power field (HPF).

Assessment of lung cell apoptosis and proliferation

In order to assess cell apoptosis and proliferation, paraffin-embedded sections were stained with rabbit polyclonal cleaved caspase-3 (CC3; 1:100, Cell Signaling Technology, Danvers, MA) and Ki67 (1:100, Abcam, Cambridge, MA) antibodies, respectively. Cell nuclei were stained with DAPI (Vector Laboratories). A blinded observer evaluated five randomly selected, non-overlapping parenchymal fields from lung sections of each animal. Lung cell apoptotic and proliferation indices were determined by quantifying the percentage of CC3- and Ki67-positive cells, respectively, in each HPF.

Assessment of pulmonary vascular remodeling

Paraffin-embedded lung sections were stained with polyclonal rabbit anti-human vWF (1:200) and monoclonal mouse anti-alpha smooth muscle actin antibodies (α-SMA; 1:500, Sigma-Aldrich, St Louis, MO). Medial wall thickness of partially and fully muscular pulmonary vessels (20–50 µm) was determined by using the formula: 2 (MT)/ED, where MT is the distance between the outer and inner boundary of the α-SMA-positive medial layer and ED is the external diameter. Approximately 20 randomly chosen vessels were evaluated per slide by a blinded observer. The percentage of peripheral pulmonary vessels (20–50 µm in diameter) stained with α-SMA >50% of the circumference was determined from ten random images on each lung section.

Assessment of lung inflammation

Lung macrophage infiltration was assessed by immunostaining lung sections with a rat monoclonal antibody to MAC-3 (1:20, BD Biosciences, San Jose, CA). The number of MAC-3-positive cells in the alveolar air spaces was determined by evaluating 10 random images taken with the ×40 objective on each slide and quantifying the number of MAC-3-positive cells per HPF. Lung myeloperoxidase (MPO) activity, interleukin (IL)-6, and TNF-α concentration in homogenized lung samples were determined by enzyme-linked immunosorbent assay (ELISA). MPO, IL-6, and TNF-α ELISA kits were obtained from Abcam (Cambridge, MA).

Western blot analysis

The protein expression of monocyte chemoattractant protein (MCP), NF-kβ (total and phosphorylated), and TSG-6 in lung homogenates were determined by western blot as previously described.[24] The polyclonal antibodies for MCP (1:500), NF-kβ (1:500), and phosphorylated NF-kβ (1:500) were obtained from Cell Signaling Technology and the mouse monoclonal antibody to TSG-6 (1:500) was obtained from Santa Cruz Biotechnology (Dallas, TX). β-Actin

was used as the normalizing protein (1:10,000, Sigma-Aldrich). Briefly, lung homogenates were separated by 10% sodium dodecyl sulfate-polyacrylamide gel electrophoresis, transferred to nitrocellulose membranes, and blocked overnight at 4 °C in 5% bovine serum albumin. Immunodetection was performed by incubating the membranes with the primary antibodies diluted in blocking buffer for 1 h at room temperature. After washing, a semilumiscent horseradish peroxidase substrate was diluted in blocking buffer and applied for 60 min. Band intensity was quantified with the Quantity One software (Bio-Rad, Hercules, CA).

Real-time reverse transcription polymerase chain reaction (RT-PCR)
Lung TSG-6 expression was determined by real-time RT-PCR. RNA from lung tissue was extracted (RNeasy Midi Kit; Qiagen, Inc. Valencia, CA) and reverse-transcribed. Real-time RT-PCR was performed on an ABI Fast 7500 system (Applied Biosystems, Foster City, CA). Primers for TSG-6 and 18S (as an internal control) were pre-developed by Applied Biosystems. The relative mRNA expression of human and rat TSG-6 was normalized to 18S expression.

Statistical analysis
Data are expressed as mean ± standard deviation and were analyzed by two-way analysis of variance with post hoc analysis (Holm–Sidak). $P \le 0.05$ was considered as statistically significant. Statistical analysis was performed using the Sigma Stat software (SyStat Software, San Jose, CA).

RESULTS

Lung TSG-6 expression increases with postnatal age
We first sought to ascertain the developmental expression of TSG-6 in the neonatal rat lung and the effect of neonatal hyperoxia exposure on lung TSG-6 expression. Whole-lung lysates were obtained from newborn rat pups exposed to RA or hyperoxia (85% O_2) for 3, 5, and 14 days. Lung TSG-6 mRNA and protein expression were determined by RT-PCR and western blot analysis, respectively.

TSG-6 gene and protein expression increased with postnatal age (Fig. 1). As compared to 3-day-old pups, there was 15-fold increase in lung TSG-6 gene expression in the lungs of 5- and 14-day-old rats (Fig. 1a). Consistent with this finding, western blot analysis also revealed a significant increase in lung TSG-6 protein expression with postnatal age.

While there was no increase in lung TSG-6 gene expression between RA and hyperoxia rats at any postnatal age, 5-day-old rats had a modest increase in lung TSG-6 protein expression when compared with the RA rats (Fig. 1b, c).

Lung human TSG-6 expression in AdTSG-6-treated pups
Next, we determined whether IT administration of AdTSG-6 would be an effective technique to deliver AdTSG-6 to the neonatal lung. Successful adenoviral transfer of TSG-6 was determined by evaluating lung human TSG-6 mRNA expression by real-time RT-PCR. As compared to IT PL-treated rat pups, there was an almost 2.5-fold increase in human TSG-6 mRNA expression in the lungs of 14-day-old RA and hyperoxic rat

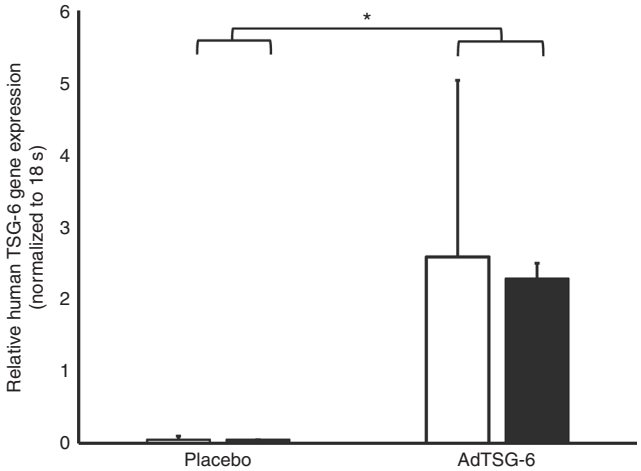

Fig. 2 Increased human TSG-6 mRNA expression in AdTSG-6-treated pups. Human TSG-6 mRNA is increased in RA and hyperoxic animals who received intra-tracheal (IT) AdTSG-6 (*$P < 0.05$; placebo vs AdTSG-6; $N = 5$/group). White bars are normoxia and black bars are hyperoxia

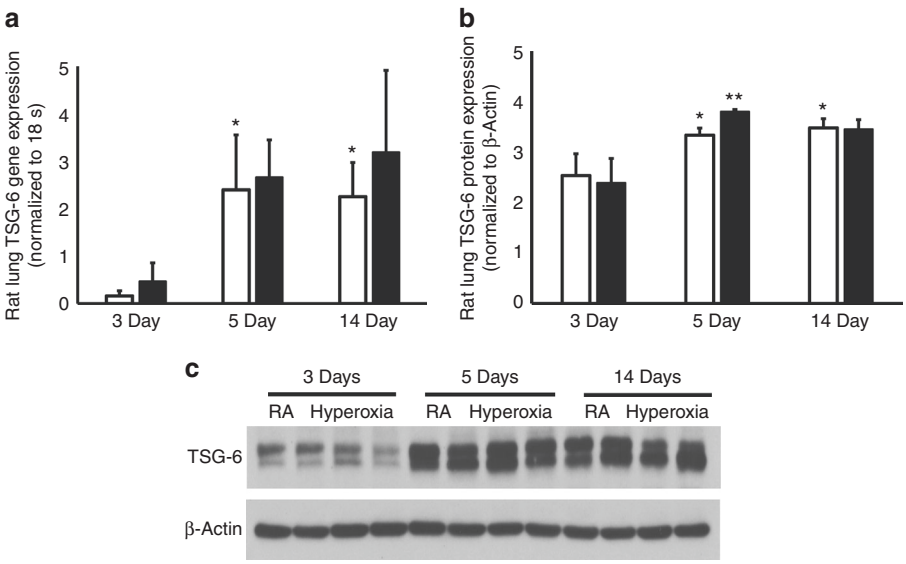

Fig. 1 Developmental expression of TSG-6 mRNA and protein in newborn rat lungs. Increased lung TSG-6 mRNA (**a**) and protein expression (**b**) with postnatal age. Lung TSG-6 protein expression was also increased following 5 days of hyperoxia exposure, ($P < 0.05$; *RA 3 Day vs RA 5 Day and RA 3 Day vs RA 14 Day, **RA vs hyperoxia 5 Days; $N = 3$–6/group). **c** A representative western blot is shown in the lower panel. TSG-6 protein expression is normalized to β-Actin. *RA* room air. White bars indicate room air and black bars indicate hyperoxia

pups who received IT AdTSG-6 ($P < 0.05$; PL vs TSG-6; $N = 5$/group), Fig. 2.

IT AdTSG-6 decreases NF-kβ expression

The transcription factor NF-kβ regulates cellular responses to inflammatory and oxidant stress via discrete signaling pathways. Significantly higher NF-kβ concentration is evident in the tracheal aspirates of preterm infants who develop BPD[19] and TSG-6 modulates NF-kβ activation.[27] Thus we next evaluated the effect of IT AdTSG-6 on NF-kβ activation in lung lysates. Whereas hyperoxic PL-treated pups had a significant increase in phosphorylated NF-kβ expression, this was reduced by two-fold following administration of IT AdTSG-6 ($P < 0.05$; hyperoxia-PL vs hyperoxia-AdTSG-6; $N = 5$/group), Fig. 3.

IT AdTSG-6 decreases lung inflammation

Since NF-kβ modulates pro-inflammatory signaling, we next questioned whether IT AdTSG-6 would decrease lung inflammation in experimental BPD. There was no difference in lung macrophage infiltration in pups exposed to RA (Fig. 4a, b). In contrast, hyperoxia-exposed PL-treated pups had a significant increase in the number of MAC-3-positive cells per HPF and this was reduced in the pups who received IT AdTSG-6 (5.4 ± 0.8 vs

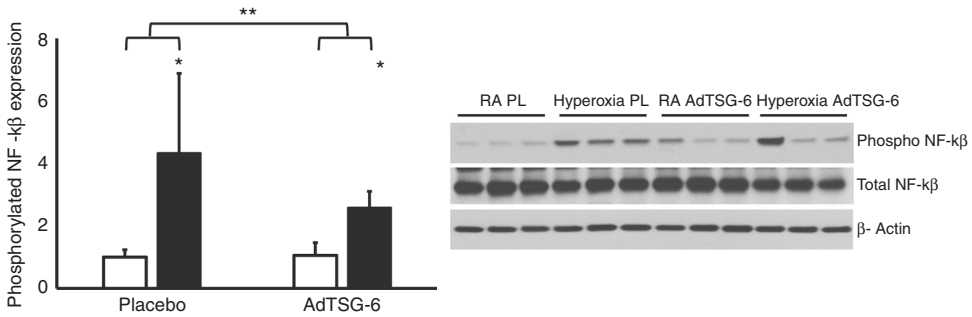

Fig. 3 Intra-tracheal (IT) AdTSG-6 decreases NF-kβ expression in experimental BPD. Decreased phosphorylated NF-kβ expression in the lungs of hyperoxic IT AdTSG-6-treated pups ($P < 0.05$; *RA vs hyperoxia, **hyperoxia-PL vs hyperoxia-AdTSG-6; $N = 5$/group). A representative western blot is shown in the right panel. Phosphorylated NF-kβ expression is normalized to total NF-kβ. White bars indicate room air and black bars indicate hyperoxia. *RA* room air, *PL* placebo

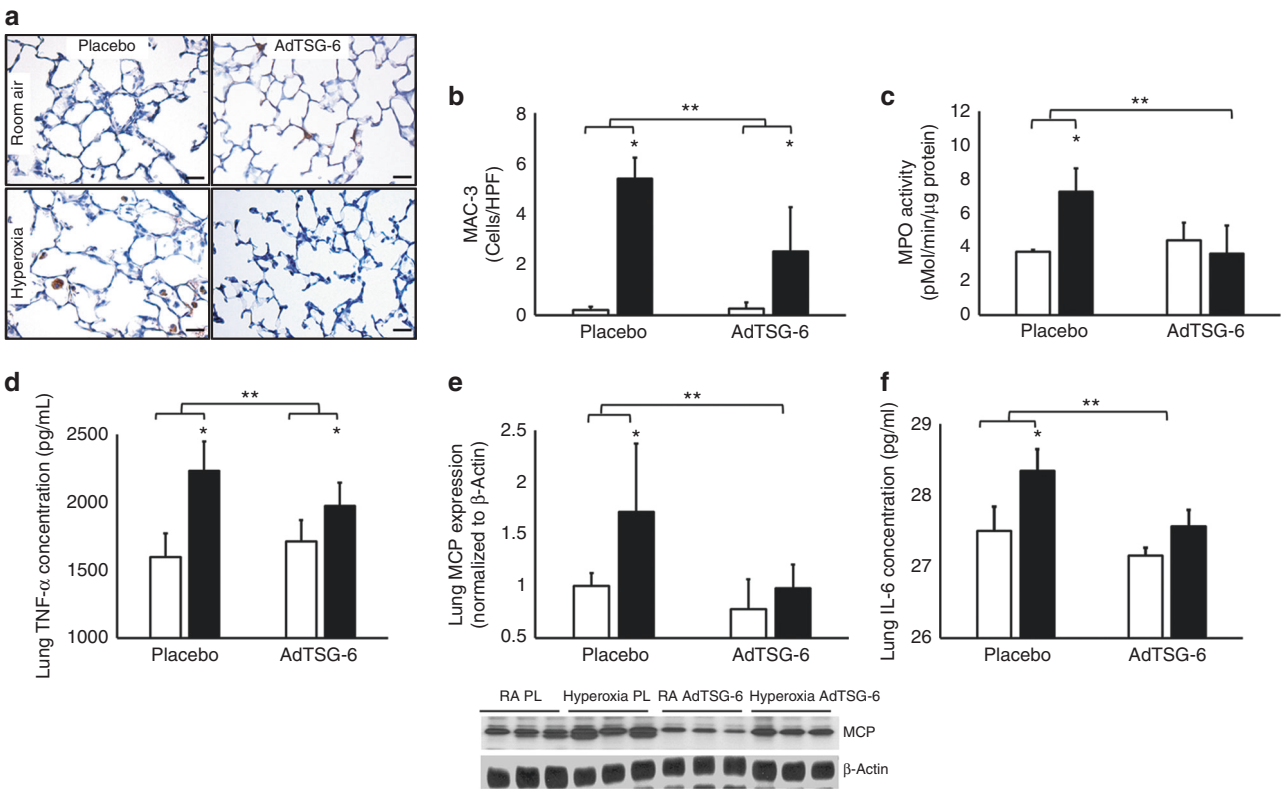

Fig. 4 IT AdTSG-6 decreases lung inflammation in experimental BPD. **a** Decreased MAC-3-positive cells (brown staining) in hyperoxia-AdTSG-6-treated pups. Magnification ×200. Scale bar is 100 µm. **b** Significantly decreased lung MAC-3-positive cells/high power field (HPF), **c** myeloperoxidase (MPO) activity, **d** tumor necrosis factor-α (TNF-α) concentration, **e** monocyte chemo-attractant protein (MCP) expression, and **f** IL-6 concentration in hyperoxic pups who received IT Ad-TSG-6, ($P < 0.05$; *RA vs hyperoxia, **hyperoxia-PL vs hyperoxia-AdTSG-6; $N = 5$/group). White bars are normoxia and black bars are hyperoxia. MCP expression is normalized to β-Actin. *RA* room air, *PL* placebo

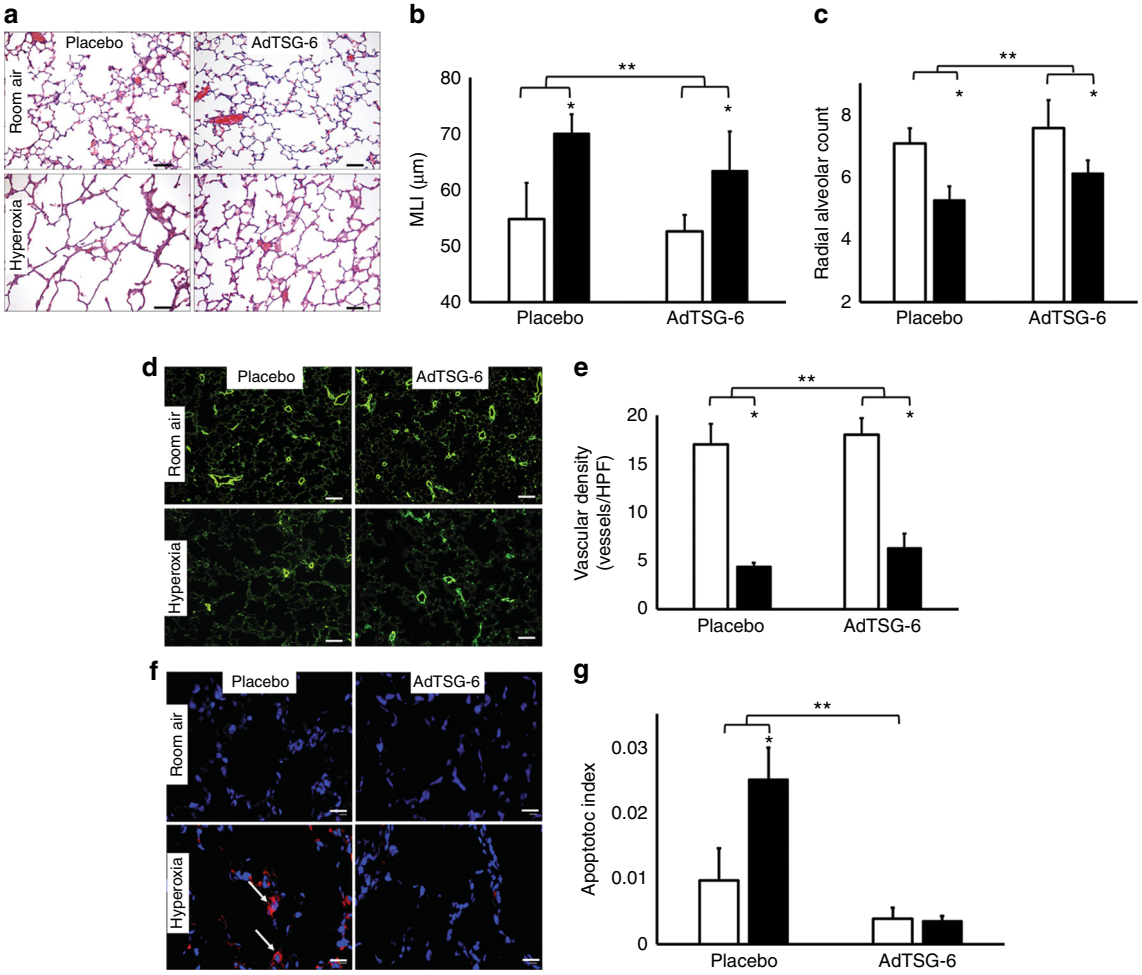

Fig. 5 IT AdTSG-6 improves alveolar structure, increases lung vascular density, and reduces apoptosis in experimental BPD. **a** Hematoxylin and eosin-stained lung sections demonstrating improved alveolar structure in hyperoxia-exposed pups treated with AdTSG-6. IT AdTSG-6 significantly **b** decreased mean linear intercept (MLI) and **c** increased radial alveolar count (RAC) in hyperoxia-exposed pups. **d** Lung sections stained with von Willebrand Factor (green) demonstrating increased lung vascular density in hyperoxia-exposed pups treated with IT AdTSG-6. **e** Increased vessels per high-power field (HPF) in IT AdTSG-6-treated hyperoxia-exposed pups. **f** Decreased cleaved caspase-3-positive cells (red) in AdTSG-6-treated hyperoxia-exposed pups. White arrows are cleaved caspase-3-positive cells. **g** Decreased apoptotic index in AdTSG-6 hyperoxia-treated pups ($P < 0.05$; *RA vs hyperoxia, **hyperoxia-PL vs hyperoxia-AdTSG-6; $N = 5$–8/group). White bars are RA and black bars are hyperoxia. Original magnification ×200. Scale bars are 100 μm

2.5 ± 1.7 cells/HPF, hyperoxia-PL vs hyperoxia-AdTSG-6; $P < 0.05$; $N = 5$/group).

MPO is a lysosomal protein stored in neutrophil granules, which is released into the extracellular space during neutrophil degranulation. There was no difference in MPO activity in pups exposed to RA. While hyperoxia-exposed PL-treated pups had a significant increase in lung MPO activity, this was reduced in the pups who received AdTSG-6 (7.3 ± 1.4 vs 3.6 ± 1.7 pmol/min/μg protein, hyperoxia-PL vs hyperoxia-AdTSG-6; $P < 0.05$; $N = 5$/group), Fig. 4c. This was accompanied by a reduction in lung TNF-α concentration (2234 ± 213 vs 1976 ± 167 pg/ml, hyperoxia-PL vs hyperoxia-AdTSG-6; $P < 0.05$; $N = 5$/group), MCP expression, and IL-6 concentration ($P < 0.05$; hyperoxia-PL vs hyperoxia-AdTSG-6; $N = 5$/group), Fig. 4d–f.

IT AdTSG-6 improves lung alveolarization, increases vascular density and decreases cell death in experimental BPD

Since inflammation plays a key role in cell apoptosis, alveolar simplification, and vascular pruning in BPD, we next determined whether AdTSG-6 would improve lung alveolarization and angiogenesis and decrease apoptosis. Hematoxylin and eosin-stained lung sections from RA and hyperoxia-exposed pups are shown in Fig. 5a. Compared to PL-treated RA-exposed pups, hyperoxia PL-treated pups had worsened alveolarization as evidenced by decreased RAC and increased MLI (55 ± 6 vs 70 ± 3 μm, RA vs hyperoxia-PL; $P < 0.05$; $N = 5$-8/group). Administration of IT AdTSG-6 significantly decreased MLI (70 ± 3 vs 63 ± 7 μm, hyperoxia-PL vs hyperoxia-AdTSG-6; $P < 0.05$; $N = 5$-8/group) and increased RAC, Fig. 5b, c, suggesting that IT AdTSG-6 improves alveolar structure in experimental BPD.

Angiogenesis was determined by staining of lung sections with vWF, Fig. 5d. There was no difference in vascular density between the RA groups. As compared to RA-PL, exposure to hyperoxia significantly decreased vascular density (17 ± 2 vs 4 ± 1 vessels per HPF, RA vs hyperoxia-PL; $P < 0.05$; $N = 5$–8/group). In contrast, administration of IT AdTSG-6 to hyperoxic pups improved angiogenesis (4 ± 1 vs 6 ± 2 vessels per HPF, hyperoxia-PL vs hyperoxia-AdTSG-6; $P < 0.05$; $N = 5$–8/group), Fig. 5e.

Moreover, whereas hyperoxia PL-treated pups had increased lung parenchymal apoptosis evidenced by increased cleaved caspase-3-positive cells, this was significantly diminished following AdTSG-6 administration (Fig. 5f, g). There was no difference in cell proliferation between the hyperoxia groups.

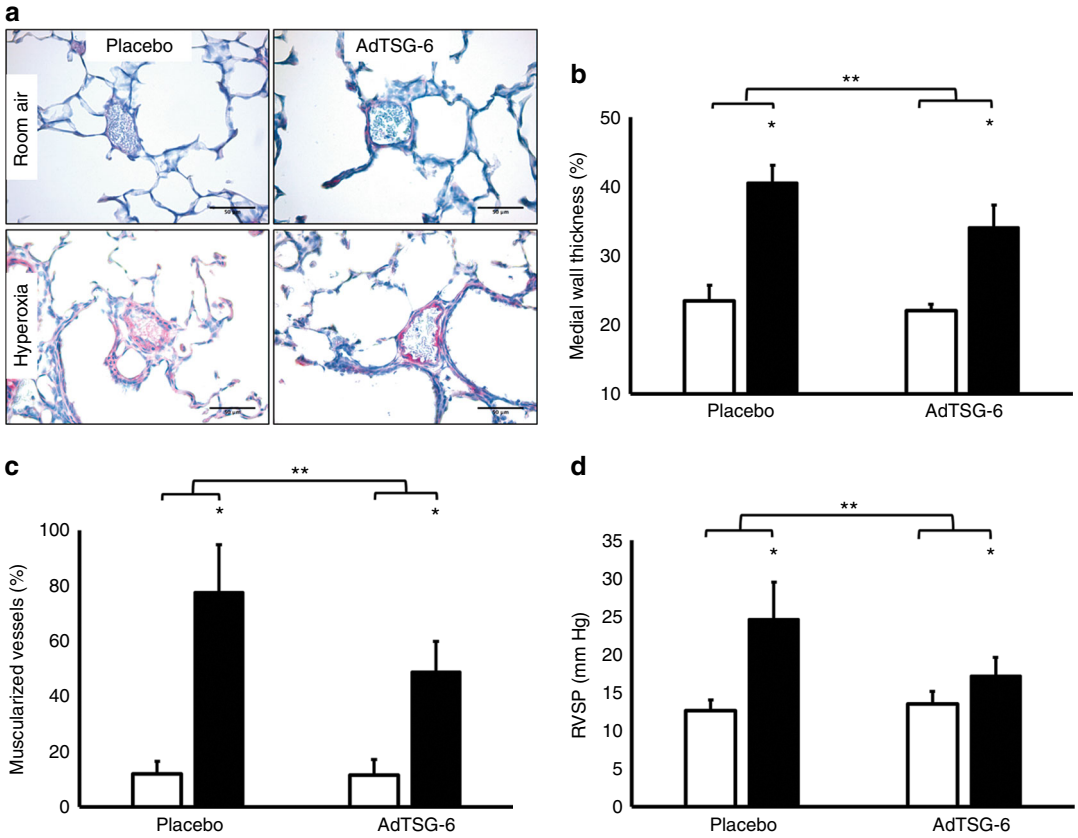

Fig. 6 IT AdTSG-6 decreases pulmonary vascular remodeling and attenuates pulmonary hypertension in experimental BPD. **a** Lung sections stained with smooth muscle actin (pink) demonstrating reduced medial wall thickness of pulmonary vessels following administration of IT AdTSG-6 to hyperoxia-exposed pups. Original magnification ×400. Scale bars are 50 μm. **b** IT AdTSG-6 decreased the medial wall thickness, **c** percentage of muscularized pulmonary vessels, and **d** right ventricular systolic pressure (RVSP) in hyperoxia-exposed pups ($P < 0.05$; *RA vs hyperoxia, **hyperoxia-PL vs hyperoxia-AdTSG-6; $N = 8$/group). White bars are RA and black bars are hyperoxia

IT AdTSG-6 decreases vascular remodeling and attenuates PH in experimental BPD

We next evaluated the effect of IT AdTSG-6 on PH and vascular remodeling. Following immunostaining of lung sections with vWF and α-SMA, pulmonary vascular remodeling was determined by quantifying the medial wall thickness and percentage of muscularized vessels (Fig. 6a–d). IT AdTSG-6 markedly decreased pulmonary vascular remodeling in hyperoxic pups as evidenced by decreased medial wall thickness (41 ± 3 vs 34 ± 3%, hyperoxia-PL vs hyperoxia-AdTSG-6; $P < 0.05$, $N = 8$/group) and reduced percentage of fully muscularized vessels (78 ± 17 vs 49 ± 11%, hyperoxia-PL vs hyperoxia-AdTSG-6; $P < 0.05$, $N = 8$/group), Fig. 6b, c. Moreover, while there was an increase in RVSP in hyperoxia-PL exposed pups (13 ± 1 vs 25 ± 5 mm Hg, RA vs hyperoxia-PL; $P < 0.05$, $N = 8$/group), administration of IT AdTSG-6 markedly reduced RVSP (25 ± 5 vs 17 ± 2 mm Hg, hyperoxia-PL vs hyperoxia-AdTSG-6; $P < 0.05$, $N = 8$/group), Fig. 6d. Together, these findings demonstrate that IT AdTSG-6 attenuates PH and vascular remodeling in experimental BPD.

DISCUSSION

Inflammation is one of the main insults, which causes aberrant lung development and remodeling in preterm infants with BPD. In the present study, we demonstrate that IT administration of an adenovirus overexpressing TSG-6 markedly suppresses lung inflammation, improves lung structure, decreases apoptosis, and attenuates PH in experimental BPD. These findings have important implications as it suggests that strategies that increase lung TSG-6 expression may have therapeutic efficacy in BPD.

TSG-6 is a hyaluronan-binding protein, which is produced by several cells in response to inflammation.[8] While most reports suggest that there is sparse TSG-6 constitutive expression, in our present study, we demonstrate that TSG-6 is constitutively expressed in the developing rat lungs and its expression increases with postnatal age.[28] This disparity may potentially be species or developmentally related. However, tissues with a risk of high oxidative stress and inflammation may constitutively express TSG-6.[28] Interestingly, rat pups exposed to hyperoxia showed no significant change in TSG-6 expression at the mRNA level and the increase in lung TSG-6 protein expression at 5 days of hyperoxia exposure was modest. Although the latter finding is consistent with prior studies that demonstrate an increased TSG-6 expression in inflamed tissues, potentially the response in our study may have been sub-optimal, thus limiting its anti-inflammatory effects. We postulate that this weaker response may be due to immaturity of the neonatal immune system or potentially species related.

The mechanisms by which TSG-6 modulate inflammation are complex. TSG-6 is composed mainly of contiguous protein chains known as Link and CUB (complement protein subcomponents C1r/C1s, urchin embryonic growth factor, and bone morphogenetic protein) modules.[17,29] Link module binds various glycosaminoglycans, including hyaluronan, chondroitin sulfate, heparin, and heparin sulfate.[17] TSG-6 via its Link module inhibits neutrophil adhesion and migration in a hyaluronan and inter-alpha-inhibitor-dependent manner.[30] In addition, TSG-6 modulates the interaction of hyaluronan with CD44, a receptor expressed on macrophages.[18] This interaction of TSG-6 with CD44 decreases NF-kβ pro-inflammatory signaling. In a recent study of lipopolysaccharide (LPS)-induced lung injury, TSG-6 suppressed lung inflammation by

shifting macrophages from a pro-inflammatory to anti-inflammatory phenotype and this was secondary to suppression of TLR4/NF-kB signaling and signal transducer and activator of transcription factor 1 (STAT1) and STAT3 activation.[18]

In our present study, hyperoxia PL-treated pups had a significant increase in phosphorylated NF-kβ expression and this was decreased following administration of IT AdTSG-6. Reduced markers of lung inflammation also accompanied the TSG-6-induced reduction in NF-kβ activation. NF-kβ is known to regulate the expression of many pro-inflammatory genes associated with the development of BPD[19] but the role of NF-kβ in BPD is controversial. Whereas activation of NF-kβ inhibits lung morphogenesis,[31] other studies suggest that NF-kβ plays an essential role in physiologic lung development, mediating both alveolarization and angiogenesis.[32] Our present findings are, however, consistent with other studies, which have demonstrated that TSG-6 reduction in NF-kβ signaling results in decreased inflammation.[27] Moreover, administration of recombinant TSG-6 decreases inflammatory cytokines in LPS-induced brain inflammation[28] and significantly suppresses LPS-induced upregulation of MCP-1, intercellular adhesion molecule-1, and vascular adhesion molecule-1 in human endothelial cells.[33]

In our experimental model of BPD, TSG-6 also decreased lung cell apoptosis and improved alveolar structure. Prior studies have demonstrated that inflammation increases lung apoptosis and impairs alveolarization.[34,35] Prenatal inflammation induced by systemic LPS exposure in pregnant mice delays alveolarization in newborn mice[34] and postnatal LPS exposure increases inflammatory responses and impairs alveolar development.[36] Our present findings demonstrating that TSG-6-mediated improvement in inflammation decreases apoptosis and promotes restoration of alveolar structure are in keeping with other studies demonstrating the alveolar regenerative effects of anti-inflammatory therapies.[23]

Vascular pruning is another characteristic feature of BPD. Infants with BPD have decreased number and abnormal distribution of pulmonary vessels.[37] Parallel increases in vascular growth are closely synchronized with alveolarization. Our present study demonstrated that the reduction in vascular density in hyperoxic pups was modestly improved by the administration of IT AdTSG-6. Other studies have demonstrated that prenatal exposure to infection increases cytokine release and inhibits vascular development.[38] Additionally, postnatal production of IL-1β disrupts capillary development and inhibits the production of vascular endothelial growth factor in the lungs of infant mice.[39]

Another important finding in our study was the improvement in PH in pups who received IT AdTSG-6. PH contributes significantly to the high morbidity and mortality in BPD. There are multiple factors that play a role in the development of PH. These include pulmonary vascular remodeling, decreased angiogenesis, increased vascular tone, and altered vasoreactivity. Exposure of vascular smooth muscle cells to inflammatory cytokines increases smooth muscle proliferation and vascular remodeling.[40] We postulate that the improvement in vascular remodeling and PH in our present study was secondary to the decreased inflammatory cytokine production following administration of IT AdTSG-6.

There were several limitations to our study. This hyperoxic rodent model corresponds to the saccular to alveolar stages of human lung development model and most preterm infants who develop BPD are in the late canalicular to early saccular stages of lung development. In addition, although hyperoxia is a significant contributor to the pathogenesis of BPD, we recognize that the disease is multifactorial and thus this therapy will need to be evaluated in multiple models. Our present model also utilized a relatively high oxygen concentration, which mimics severe BPD, and thus further studies evaluating a milder form of BPD will be necessary. We also recognize that we only evaluated early administration of TSG-6 and thus it will be critical to perform further studies evaluating later dosing and its effects on chronic lung inflammation. In addition, whereas the effects on lung inflammation with IT AdTSG-6 were marked, the effects on lung structure and angiogenesis were modest. We speculate that these differential effects may be dose related or potentially secondary to NF-kβ pleiotropic signaling.

In conclusion, our study demonstrates that adenoviral-mediated gene transfer of TSG-6 robustly decreases lung inflammation, improves lung structure, reduces apoptosis, and attenuates PH and vascular remodeling in experimental BPD. Although further investigations will be needed, this study suggests that therapies, which augment lung TSG-6 expression, may be potentially efficacious for the treatment of BPD.

ADDITIONAL INFORMATION

Competing interests: The authors declare no competing interests.

Publisher's note: Springer Nature remains neutral with regard to jurisdictional claims in published maps and institutional affiliations.

REFERENCES

1. Coalson, J. J. Pathology of new bronchopulmonary dysplasia. *Semin. Neonatol.* **8**, 73–81 (2003).
2. Walsh, M. C. et al. Impact of a physiologic definition on bronchopulmonary dysplasia rates. *Pediatrics* **114**, 1305–1311 (2004).
3. Stoll, B. J. et al. Neonatal outcomes of extremely preterm infants from the NICHD Neonatal Research Network. *Pediatrics* **126**, 443–456 (2010).
4. Stoll, B. J. et al. Trends in care practices, morbidity, and mortality of extremely preterm neonates, 1993–2012. *JAMA* **314**, 1039–1051 (2015).
5. Jobe, A. H. & Bancalari, E. Bronchopulmonary dysplasia. *Am. J. Respir. Crit. Care Med.* **163**, 1723–1729 (2001).
6. Munshi, U. K., Niu, J. O., Siddiq, M. M. & Parton, L. A. Elevation of interleukin-8 and interleukin-6 precedes the influx of neutrophils in tracheal aspirates from preterm infants who develop bronchopulmonary dysplasia. *Pediatr. Pulmonol.* **24**, 331–336 (1997).
7. Lee, T. H., Wisniewski, H. G. & Vilcek, J. A novel secretory tumor necrosis factor-inducible protein (TSG-6) is a member of the family of hyaluronate binding proteins, closely related to the adhesion receptor CD44. *J. Cell Biol.* **116**, 545–557 (1992).
8. Maina, V. et al. Coregulation in human leukocytes of the long pentraxin PTX3 and TSG-6. *J. Leuk. Biol.* **86**, 123–132 (2009).
9. Coulson-Thomas, V. J. et al. Tumor necrosis factor-stimulated gene-6 (TSG-6) is constitutively expressed in adult central nervous system (CNS) and associated with astrocyte-mediated glial scar formation following spinal cord injury. *J. Biol. Chem.* **291**, 19939–19952 (2016).
10. Forteza, R. et al. TSG-6 potentiates the antitissue kallikrein activity of inter–α-inhibitor through bikunin release. *Am. J. Resp. Cell Mol. Biol.* **36**, 20–31 (2007).
11. Wisniewski, H. G. & Vilcek, J. TSG-6: An IL-1/TNF-inducible protein with anti-inflammatory activity. *Cytokine Growth Factor Rev.* **8**, 143–156 (1997).
12. Lee, R. H. et al. Intravenous hMSCs improve myocardial infarction in mice because cells embolized in lung are activated to secrete the anti-inflammatory protein TSG-6. *Cell Stem Cell* **5**, 54–63 (2009).
13. Liu, L. et al. TSG-6 secreted by human umbilical cord-MSCs attenuates severe burn-induced excessive inflammation via inhibiting activations of p38 and JNK signaling. *Sci. Rep.* **6**, 30121 (2016).
14. Lee, R. T. et al. Mechanical strain induces specific changes in the synthesis and organization of proteoglycans by vascular smooth muscle cells. *J. Biol. Chem.* **276**, 13847–13851 (2001).
15. Margerie, D. et al. Complexity of IL-1 beta induced gene expression pattern in human articular chondrocytes. *Osteoarthr. Cartil.* **5**, 129–138 (1997).
16. Milner, C. M., Higman, V. A. & Day, A. J. TSG-6: a pluripotent inflammatory mediator? *Biochem. Soc. Trans.* **34**, 446–450 (2006).
17. Parkar, A. A. & Day, A. J. Overlapping sites on the link module of human TSG-6 mediate binding to hyaluronan and chrondroitin-4-sulphate. *FEBS Lett.* **410**, 413–417 (1997).
18. Mittal, M. et al. TNFα-stimulated gene-6 (TSG6) activates macrophage phenotype transition to prevent inflammatory lung injury. *Proc. Natl. Acad. Sci. USA* **113**, E8151–E8158 (2016).
19. Bourbia, A., Cruz, M. A. & Rozycki, H. J. Nf-κb in tracheal lavage fluid from intubated premature infants: association with inflammation, oxygen, and outcome. *Arch. Dis. Child Fetal Neonatal Ed.* **91**, F36–F39 (2006).

20. Foskett, A. M. et al. Phase-directed therapy: TSG-6 targeted to early inflammation improves bleomycin-injured lungs. *Am. J. Physiol. Lung Cell Mol. Physiol.* **306**, L120–L131 (2014).
21. Swaidani, S. et al. TSG-6 protein is crucial for the development of pulmonary hyaluronan deposition, eosinophilia, and airway hyperresponsiveness in a murine model of asthma. *J. Biol. Chem.* **288**, 412–422 (2013).
22. Oh, J. Y. et al. Anti-inflammatory protein TSG-6 reduces inflammatory damage to the cornea following chemical and mechanical injury. *Proc. Natl. Acad. Sci. USA* **107**, 16875–16880 (2010).
23. Chaubey, S. et al. Early gestational mesenchymal stem cell secretome attenuates experimental bronchopulmonary dysplasia in part via exosome-associated factor TSG-6. *Stem Cell Res. Ther.* **9**, 173 (2018).
24. Young, K. C. et al. Inhibition of the SDF-1/CXCR4 axis attenuates neonatal hypoxia-induced pulmonary hypertension. *Circ. Res.* **104**, 1293–1301 (2009).
25. Miranda, L. F. et al. Stem cell factor improves lung recovery in rats following neonatal hyperoxia-induced lung injury. *Pediatr. Res.* **74**, 682–688 (2013).
26. Cooney, T. P. & Thurlbeck, W. M. The radial alveolar count method of Emery and Mithal: a reappraisal 2–intrauterine and early postnatal lung growth. *Thorax* **37**, 580–583 (1982).
27. Choi, H., Lee, R. H., Bazhanov, N., Oh, J. Y. & Prockop, D. J. Anti-inflammatory protein TSG-6 secreted by activated mscs attenuates zymosan-induced mouse peritonitis by decreasing TLR2/NF-kappab signaling in resident macrophages. *Blood* **118**, 330–338 (2011).
28. Bertling, F. et al. Tumor necrosis factor-inducible gene 6 protein: a novel neuroprotective factor against inflammation-induced developmental brain injury. *Exp. Neurol.* **279**, 283–289 (2016).
29. Kohda, D. et al. Solution structure of the link module: a hyaluronan-binding domain involved in extracellular matrix stability and cell migration. *Cell* **86**, 767–775 (1996).
30. Getting, S. J. et al. The link module from human TSG-6 inhibits neutrophil migration in a hyaluronan- and inter-alpha -inhibitor-independent manner. *J. Biol. Chem.* **277**, 51068–51076 (2002).
31. Benjamin, J. T. et al. Nf-κb activation limits airway branching through inhibition of sp1-mediated fibroblast growth factor-10 expression. *J. Immunol.* **185**, 4896–4903 (2010).
32. Iosef, C. et al. Inhibiting NF-κb in the developing lung disrupts angiogenesis and alveolarization. *Am. J. Physiol. Lung Cell Mol. Physiol.* **302**, L1023–L1036 (2012).
33. Watanabe, R. et al. Atheroprotective effects of tumor necrosis factor–stimulated gene-6. JACC: basic to translational. *Science* **1**, 494–509 (2016).
34. Velten, M., Heyob, K. M., Rogers, L. K. & Welty, S. E. Deficits in lung alveolarization and function after systemic maternal inflammation and neonatal hyperoxia exposure. *J. Appl. Physiol. (1985)* **108**, 1347–1356 (2010).
35. Ward, N. S. et al. Interleukin-6–induced protection in hyperoxic acute lung injury. *Am. J. Resp. Cell Mol. Biol.* **22**, 535–542 (2000).
36. Franco, M. L. et al. Lps-induced lung injury in neonatal rats: changes in gelatinase activities and consequences on lung growth. *Am. J. Physiol. Lung Cell Mol. Physiol.* **282**, L491–L500 (2002).
37. Bhatt, A. J. et al. Disrupted pulmonary vasculature and decreased vascular endothelial growth factor, Flt-1, and tie-2 in human infants dying with bronchopulmonary dysplasia. *Am. J. Resp. Crit. Care Med.* **164**, 1971–1980 (2001).
38. Kallapur, S. G., Jobe, A. H., Ikegami, M. & Bachurski, C. J. Increased IP-10 and MIG expression after intra-amniotic endotoxin in preterm lamb lung. *Am. J. Respir. Crit. Care Med.* **167**, 779–786 (2003).
39. Bry, K., Whitsett, J. A. & Lappalainen, U. Il-1β disrupts postnatal lung morphogenesis in the mouse. *Am. J. Respir. Cell Mol. Biol.* **36**, 32–42 (2007).
40. Coflesky, J. T., Adler, K. B., Woodcock-Mitchell, J., Mitchell, J. & Evans, J. N. Proliferative changes in the pulmonary arterial wall during short-term hyperoxic injury to the lung. *Am. J. Pathol.* **132**, 563–573 (1988).